HHS Public Access

Author manuscript

Forensic Sci Int. Author manuscript; available in PMC 2020 August 01.

Published in final edited form as:

Forensic Sci Int. 2019 August ; 301: 289–298. doi:10.1016/j.forsciint.2019.05.042.

Functional Characterization of *SCN10A* Variants in Several Cases of Sudden Unexplained Death

Ivan Gando, MS[1], **Nori Williams, MS CGC**[5], **Glenn I. Fishman, MD**[2,3,4], **Barbara A. Sampson, MD PhD**[5], **Yingying Tang, MD PhD**[5], and **William A. Coetzee, DSc**[1,2,3]

[1]Pediatrics, New York, NY

[2]Physiology & Neuroscience, New York, NY

[3]Biochemistry and Molecular Pharmacology, New York, NY

[4]Medicine NYU School of Medicine, New York, NY

[5]Molecular Genetics Laboratory, Office of Chief Medical Examiner, New York, NY

Abstract

Background—Multiple genome-wide association studies (GWAS) and targeted gene sequencing have identified common variants in *SCN10A* in cases of PR and QRS duration abnormalities, atrial fibrillation and Brugada syndrome. The New York City Office of Chief Medical Examiner has now also identified five *SCN10A* variants of uncertain significance in six separate cases within a cohort of 330 sudden unexplained death events. The gene product of *SCN10A* is the Nav1.8 sodium channel. The purpose of this study was to characterize effects of these variants on Nav1.8 channel function to provide better information for the reclassification of these variants.

Methods and Results—Patch clamp studies were performed to assess effects of the variants on whole-cell Nav1.8 currents. We also performed RNA-seq analysis and immunofluorescence confocal microcopy to determine Nav1.8 expression in heart. We show that four of the five rare 'variants of unknown significance' (L388M, L867F, P1102S and V1518I) are associated with altered functional phenotypes. The R756W variant behaved similar to wild-type under our experimental conditions. We failed to detect Nav1.8 protein expression in immunofluorescence microscopy in rat heart. Furthermore, RNA-seq analysis failed to detect full-length *SCN10A* mRNA transcripts in human ventricle or mouse specialized cardiac conduction system, suggesting that the effect of Nav1.8 on cardiac function is likely to be extra-cardiac in origin.

Conclusions—We have demonstrated that four of five *SCN10A* variants of uncertain significance, identified in unexplained death, have deleterious effects on channel function. These

Address for correspondence: Dr. William A. Coetzee NYU School of Medicine, 450 E 29th Street, ACLS 824 New York, NY 10016, USA Tel: 1-646-501-4510 Fax: 1-212-263-5100, william.coetzee@nyu.edu.

Disclosures

None.

data extend the genetic testing of SUD cases, but significantly more clinical evidence is needed to satisfy the criteria needed to associate these variants with the onset of SUD.

Keywords

Na^+ Channels; SCN10A; Sudden unexplained death; Channelopathies

Subject terms

Sudden cardiac death; Ion channels/membrane transport

Introduction

Genetic variation in ion channel genes (channelopathies) is associated with inherited forms of arrhythmias, such as long- and short QT syndromes, Brugada syndrome, and conduction abnormalities.[1–4] Channelopathies have also been linked to sudden unexplained death (SUD) in young adults and children[1, 5–7] and it is a common assumption that cardiac rhythm disorders are involved in a subset of these cases with premature death. Multiple genome-wide association studies (GWAS) have identified common variants in *SCN10A* as potential modulators of PR and QRS durations in humans.[8–12] *SCN10A* variants have also been reported in several cases of ST-T wave amplitudes disorders[13], cardiac conduction abnormalities in hypertrophic cardiomyopathy patients[14], atrial fibrillation (AF)[15], and Brugada syndrome[16–18].

The voltage-gated sodium channel Nav1.8 subunit, encoded by the *SCN10A* gene, was initially cloned from rat DRG neurons.[19, 20]. Similar to the major cardiac Na^+ channel (Nav1.5), Nav1.8 is resistant to nanomolar concentrations of tetrodotoxin. However, Nav1.8 exhibits a more depolarized voltage dependence of inactivation and slower inactivation kinetics[19, 20] and can therefore continue to operate at depolarized voltages when most other Na^+ channels are inactivated and fail to respond to stimuli. The Nav1.8 channel is the major sodium channel in primary sensory neurons[21], especially in nociceptive neurons, where it contributes to peripheral pain processing.[21, 22] Nav1.8 is also expressed in vagal fibers, but not in the sympathetic system.[23, 24] There are also reports of Nav1.8 expression in nerve fibers and fascicles in the myocardium, in cardiac myocytes, and in the specialized cardiac conduction system.[25–27] It is therefore conceivable for *SCN10A* variants to be associated with SUD.

With the advent of next-generation sequencing techniques, molecular testing of a large ‘cardiac’ gene panel is increasingly being performed to identify genetic variants associated with SUD and SIDS.[28–31] Variants are classified according to guidelines by the American College of Medical Genetics and Genomics (ACMG), using specific standard terminologies as ‘pathogenic’, ‘likely pathogenic’, ‘uncertain significance’, ‘likely benign’, or ‘benign’.[32] The ‘pathogenic’ and ‘likely pathogenic’ designations are often used for diagnostic purposes,[31] which forms the basis for family counseling discussions. However, the computer algorithms responsible for these predictions are fallible. A recent side-by-side analysis of 23 pathogenicity computational algorithms has shown that the specificities of these tests are

generally lower than the sensitivities, with false positive rates ranging between 10–65%.[33] Moreover, the 'variants of unknown significance' (VUS), which are often found in cases of sudden death, are not helpful for diagnostic purposes. Some of these VUS negatively impact channel function, as demonstrated by our recent studies with *SCN5A* and *TRPM4* VUS.[1, 34, 35] These functional data need to be taken into account when re-interpreting reported VUS. Following a similar approach, in this study we functionally characterized five novel or rare variants of unknown significance in the *SCN10A* gene that were found in six cases of unexplained death in neonates and adults. We also assessed *SCN10A* mRNA expression in human heart and the mouse specialized cardiac conduction system. We conclude that four of the five *SCN10A* VUS (L388M, L867F, P1102S and V1518I) impact channel function. Since we were not able to detect full-length *SCN10A* transcripts in cardiac tissue, it is likely that these variants may have an extra-cardiac role.

Methods

Site-directed Mutagenesis

The human Nav1.8 cDNA (Genbank accession number NM_006514) in the pEZM61 vector (clone 1171) was obtained from GeneCopoeia (EX-I3726-M61; Rockville, MD). The Nav1.8 cDNA (without the IRES EGFP fragment) was subcloned into the pcDNA3.1(+) vector (clone 1224) with restriction cloning and sequenced. All site directed mutagenesis and sequence confirmation was performed commercially (GenScript, Piscataway, NJ). The human Navβ3 (Genbank NM_001040151, with C-terminal flag epitope) cDNA in the pcDNA3.1(+) vector was obtained from GenScript (Product ID: OHu16302D).

Cell Culture

Human Embryonic Kidney (HEK) 293 cells were cultured in Dulbecco's Modified Eagle Medium (DMEM) (Thermo Fisher Scientific, Waltham, MA), supplemented with heat-inactivated 10% Fetal Bovine Serum (FBS) and penicillin-streptomycin. Cells were grown in 35mm culture plates until 70–80% confluence was reached. Cells were transfected using the Lipofectamine 2000 reagent (Life Technologies, Carlsbad, CA) with 3 μg of total DNA: 1.4 μg of Nav1.8, 1.4 μg of Navβ3 and 0.2 μg of a GFP plasmid, to allow visualization of successfully transfected cells for patch clamping. Cells were used for patch clamping or biochemistry 48h after transfection.

Patch Clamping

Whole-cell currents were recorded at room temperature (MultiClamp 700A; Axon Instruments), low-pass filtered with an 8-pole Bessel filter (−3dB @ 1 Hz.) and digitized (2 kHz; DigiData 1550A, Axon Instruments) using pClamp v10.5 software (Molecular Devices). Patch electrodes were manufactured (Zeitz puller, Germany) using borosilicate glass (1.5 mm OD; World Precision Instruments) and had tip resistances of 2.5–3.0 MΩ when filled with (in mmol/L): 120 CsF, 10 NaCl, 10 HEPES, 10 EGTA, 10 TEA-Cl, 2 Na_2ATP and pH adjusted to 7.2 with 2N CsOH. The physiologically relevant bath solution consisted of a modified Tyrode's solution (in mmol/L): 140 NaCl, 4 KCl, 10 HEPES, 1 $MgCl_2$, 2 $CaCl_2$ and pH adjusted to 7.4 using 2N NaOH. Data were not corrected for the liquid junction potential, which was calculated to be 7.4mV. The whole-cell capacitance and

series resistance were compensated to levels greater than 80%. Currents were corrected for cell size by dividing by the cell capacitance and current densities are expressed as pA/pF.

Western Blotting

Total protein concentration was measured using BioRad Protein Assay Dye Reagent (Bio-Rad). Samples with equal amounts of total protein were mixed with sample buffer (ThermoFisher Scientific, Waltham, MA) containing 50 mM DTT and kept at room temperature prior to resolving with a 10% polyacrylamide gradient gel. After transfer to polyvinylidene difluoride (PVDF) membranes (Bio-Rad) and blocking with 5% milk in TBS-Tween (0.05%) for 1 h, blots were incubated overnight at 4°C with primary antibodies and 1 h at room temperature with secondary antibodies (dissolved in blocking buffer). Detection was with chemiluminesence (SuperSignal West Dura, Thermo Scientific, Waltham, MA) and photographic film. Immunoblots were analyze and quantified using analyzed using NIH image software (ImageJ).

Immunohistochemistry

Adult rats were sacrificed by pentobarbital overdose and the hearts were rapidly removed. All animal experiments were approved by the institutional Animal Care Review Board. Hearts were perfused at 37ºC through the aorta (Langendorff mode) with Tyrode's solution (in mM: NaCl 137, KCl 5.4, HEPES 10, $CaCl_2$ 1.8, $MgCl_2$ 1, NaH_2PO_4 0.33; pH adjusted to 7.4 with NaOH) containing pinacidil (100 μM) to cause maximal vasodilatation as to clear the vasculature of blood. Hearts were fixed by switching the perfusate to paraformaldehyde (4% in phosphate-buffered saline (PBS), pH adjusted to 7.4) for 15 minutes at room temperature. The heart was incubated in 4% paraformaldehyde overnight at 4ºC. Following fixation, the tissue was incubated overnight at 4°C in 30% sucrose in PBS. The tissue was then embedded in M1 embedding matrix (Thermo Shandon, Pittsburgh, PA) and placed on dry ice until frozen. The block containing the tissue was sectioned using a cooled (−20°C) cryostat (Microm Cryo-Star HM 560, Kalamazoo MI) at 15 μm thicknesses. The sections were transferred to Superfrost Plus slides (Fisher Scientific) for further processing.

Tissue sections were allowed to warm to room temperature. The staining protocol was carried out in a moist chamber to avoid dehydration. Blocking was performed for 60 min with Tris-buffered saline (TBS; in mM 137 NaCl, 50 Tris, 2.7 KCl, pH 7.4) containing 4% goat or donkey serum (depending on the secondary antibody being used) and 0.2% Triton X-100 at room temperature. The slides were incubated overnight at 4ºC with primary antibodies (see below) diluted in TBS containing 0.1% serum and 0.2% Triton X-100. Double or triple immunofluorescent studies were carried out by incubating the tissue sections with more than one primary antibody at the same time. Sections were washed three times for 15 min each in TBS, and incubated with fluorescently labeled secondary antibodies (see below) for 1h at room temperature. The samples were again washed three times for 15 min each in TBS. Sections were drained by blotting with filter paper and a drop of mounting medium (containing an anti-fade reagent) was added to the slides before mounting with a standard coverslip. The mounting medium was allowed to dry before the slides were imaged using a Leica PS2 confocal microscope equipped with an Argon 488nm

gas laser and Helium Neon lasers (543 and 633 lines). Most images were obtained using an emission pin hole of 1.1–1.6 AE with either a 20x (0.7 NA) or a 63x (1.2 NA) oil objective.

Antibodies

Primary antibodies used were mouse monoclonal anti-voltage-gated sodium channel (1:2000; K58/35, Sigma Aldrich, St. Louis, MO), mouse monoclonal anti-GAPDH (1:10000; GAPDH-71.1, Sigma), rabbit polyclonal anti-Nav1.5 (1:200; S0819, Sigma), rabbit polyclonal anti-Neurofilament heavy polypeptide (1:100; ab8135, Abcam, Cambridge, MA), mouse monoclonal anti-Nav1.8 (1:50; Neuromab clone N143/12), AlexaFluor 488 donkey anti-rabbit (1:200; Jackson ImmunoResearch, West Grave, PA), AlexaFluor 594 donkey anti-mouse (1:200; Jackson ImmunoResearch) and goat anti-mouse-HRP secondary (1:40000; Jackson ImmunoResearch)

RNA-seq analysis

Paired read RNA-Sequencing data from non-failing adult human heart were obtained from the Gene Expression Omnibus (GEO accession number GSE71613; samples GSM1841251, GSM1841259, GSM1841261 and GSM1841263). The sequenced reads were trimmed for adaptor sequence and for low-quality sequence, then mapped to the human hg19 whole genome using STAR on the NYU Phoenix High Performance Cluster computing facility. Output BAM files were sorted by coordinates and gene counts were produced. Index files were generated with Samtools and data were visualized with the Integrated Genomics Viewer. Splice junctions were visualized from the alignment data as Sashimi plots.

Data Analysis

Patch clamp data were analyzed using pClamp 10.5 software and plotted using OriginPro 8 (OriginLab, Northampton, MA). Current-voltage curves were produced by plotting the peak current (normalized to the cell capacitance) against the clamp step potential. To generate activation curves, peak inward currents (I_{Na}) were converted to conductance as follows: $G_{Na} = I_{Na}/(V_m - V_{rev})$, where V_m is the clamp step voltage and V_{rev} the reversal potential, which was determined for each cell. Values of G_{Na} were normalized to the maximum conductance and plotted as a function of voltage. Results are presented as mean ± standard error of the mean. Statistical comparisons were performed using Student's t-tests or an Analysis of Variance, as appropriate, and statistical significance was assumed when $p < 0.05$.

Results

SCN10A Variants Associated with SUD

The purpose of this study was to functionally classify (or reclassify if needed) *SCN10A* VUS identified in our previous work where we genetically screened ~300 cases of SUD using a cardiac arrhythmogenic testing panel[28]. In that study, in six cases of sudden death we identified one novel *SCN10A* variants (i.e. absent in the gnomAD database (which includes spans of 125,748 exome sequences and 15,708 whole-genome sequences from unrelated individuals) and four rare variants (allelic frequency between 0.0004–0.01%) (Table 1). One variant (V1518I) was present in two of the cases. All of the variants were predicted to be 'variants of unknown significance" according to the classification scheme proposed by the

by ACMG/AMP 2015 guidelines. Three of the six SUD cases were infants or young children, whereas the other three cases were adults. The circumstances of death are given in Table 1. In three of the six cases there were no other detectable variants in other genes of the testing panel, which consisted of 95 'cardiac' genes (**Table S1**). In the other three cases, VUS were also detected in some of the other study panel genes (Table 1). The Nav1.8 subunit is a product of the *SCN10A* gene and is a polypeptide with 24 transmembrane (TM) segments (Figure 1), arranged in four domains (DI to DIV) with 6 TM segments each. Each of the identified VUS were missense variants, leading to a single amino acid change in the Nav1.8 subunit (Table 1). Four of the five variants cause amino acid substitutions (L388M, R756W, L867F, V1518I) within transmembrane helixes of the Nav1.8 subunit, whereas one variant resulted in an amino acid change (P1102S) within the intracellular DII-DIII loop (Figure 1). These amino acid residues are highly conserved in Nav1.8 across species and also across other human Nav1.x subunits (Figure S1).

Developing a heterologous expression system to evaluate Nav1.8 channel function

Nav1.8 can be heterologously expressed in cells of neuronal origin such as ND7–32, Neuro-2A or SH-SY5 cells,[36–38] but we wanted to avoid using these cells since they endogenously express other types of Na^+ channels. We therefore expressed the Nav1.8 cDNA in the commonly used HEK-293 cell line. However, no whole-cell currents could be recorded, despite increasing the cDNA amount in the transfection reaction (between 500 ng and 2 ug) or increasing the time after transfection (between 24h to 72h) (Figure S2). Co-expression of Nav1.8 with Na^+ channel β subunits was reported to increase the current expression.[39] Given the association of gene variants in *SCN3B* (which codes for the Navβ3 subunit) with arrhythmogenesis,[15] we tested whether this auxiliary subunit may induce expression. Indeed, we found that co-expression of Nav1.8 with Navβ3 consistently led to small, but readily detectable whole-cell currents (Figure S2). One of the mechanisms by which Navβ3 enhanced Nav1.8 currents was to increase the Nav1.8 protein expression, which was observed in a variety of cell types (Figure S2).

Functional analysis of the SCN10A variants

The *SCN10A* variants in this study are computationally classified as 'variants of unknown significance' and their potential pathogenicity can be better assessed with functional testing. We therefore introduced these nucleotide changes into the Nav1.8 cDNA with site-directed mutagenesis and co-expressed the wild-type or variants with Navβ3 cDNA in HEK-293 cells. Whole-cell currents were recorded 48 h after transfection. Consistent with previous reports,[37] we found that Nav1.8 currents activated at around −60 mV and reached a peak at about −10 mV (Figure 2). The reversal potential is at around +60 mV, which is close to the expected Na^+ equilibrium potential under our experimental conditions. The most striking initial difference was observed with the L388M variant, which had significantly smaller current amplitudes (and was undetectable in some cases) when compared to wild-type (Figure 2). On average, the Nav1.8-L388M current density at 0 mV was reduced by ~4 fold compared to wild-type. There were no statically significant differences in the peak current density for the other variants (Figure 2C). When inspecting the inactivating portion of Nav1.8 currents, it became clear that the rate of inactivation of P1102S was significantly delayed compared to wild-type (Figure 3A). Indeed, curve-fitting of the experimental traces

recorded between −20 mV and +20 mV to a single exponential function shows that P1102S inactivated significantly slower (Figure 3B), which represents a gain-of-function phenotype.

We next constructed conductance-voltage activation curves to determine if the voltage dependence of activation is affected by any of the variants. Indeed, there was a significant depolarizing shift of the voltage dependence of activation for the R756W and V1518I variants (Figure 4A). These shifts were quite large (up to 20 mV; Figure 4B), which represents a significant loss-of-function phenotype.

Effects on protein expression

We investigated whether any of the variants affect Nav1.8 protein expression levels. Western blotting was performed with an anti-Nav antibody using lysates of transfected cells. Compared to wild-type, protein levels were higher for the R756W variant, but were significantly less for the L388M and P1102S variants (Figure 5). The decreased levels may be due to decreased protein stability and subsequent degradation. We tested this possibility using the L388M variant as proof of principle. When pre-incubating cells with the proteasome inhibitor MG132, the Nav1.8-L388M protein levels were restored to near wild-type levels (Figure 6A). We followed up with patch clamp experiments and found that MG132 similarly rescued Nav1.8-L388M currents to near wild-type levels (Figure 6 B&C).

Lack of expression of SCN10A in cardiac tissue

To investigate *SCN10A* expression in heart, we started by performing immunohistochemistry with rat tissue. As a positive control, cryosections of DRG neurons show robust Nav1.8 staining, demonstrating that the anti-Nav1.8 performs adequately in this assay (Figure 7, **top**). In contrast, Nav1.8 protein expression was not detectible in rat heart cryosections, whereas Nav1.5 expression was readily detected (Figure 7, **bottom**). We investigated *SCN10A* mRNA expression with RNA-seq, which has the ability to quantitatively analyze splice variants. Analysis of human heart ventricle samples from the GEO database demonstrates that, as expected, *SCN5A* is robustly expressed in human heart with sequence reads in each of the exons. In contrast, SCN10A is not represented. Curiously, sequence reads are present in the 3’ exons of SCN10A (exons 26 and 27) and some of these reads span to the 5’ exons of SCN5A (Figure 8). The significance of this finding is not clear at present. We finally investigated the possibility that SCN10A expression is specific to the specialized cardiac conduction system.

Since human tissue is not available, we used data obtained from Cntn2-EGFP reporter mice, where the cardiac conduction system myocytes could be isolated to high purity by fluorescence FACS sorting. Similar to the human ventricle, we could not find evidence of full-length SCN10A transcripts in the mouse conduction system (data not shown).

Discussion

Functional reclassification of the SCN10A variants of unknown significance

A number of previous studies have shown that *SCN10A* variants are associated with several types ventricular of arrhythmias.[8, 9, 11, 15–18, 27, 40, 41] Two approaches have emerged from

these studies in an attempt to understand how these variants may lead to cardiac dysfunction. In a genome-wide association study (GWAS), several loci were found to be associated with QRS duration, including a variant (rs6801957) that mapped to an enhancer region of *SCN10A*.[41] Interestingly, this variant was found to strongly regulate cardiac Na^+ channel (*SCN5A*) gene expression, which might explain how this variant links with cardiac defects and arrhythmias. Since the variants identified in our study are within the *SCN10A* coding region, they are unlikely to work through this mechanism. In a second approach, some investigators have worked on the assumption that Nav1.8 and Nav1.5 are both expressed in cardiomyocytes, and that Nav1.8 variants can affect the function of the cardiac Nav1.5 channel. Therefore, in a study analyzing *SCN10A* variants found in patents with Brugada syndrome, mutant Nav1.8 were co-expressed with Nav1.5 in HEK-293 cells, and dysfunction of Nav1.5 was used as a readout.[18] In our studies we were not able to detect Nav.8 protein or full-length mRNA transcripts in hearts, and we have therefore decided not to follow this co-expression approach. Instead, we developed a heterologous expression system (Nav1.8 co-expressed with Navβ3 in HEK-293 cells) that allowed us to study the channel directly. These studies demonstrated that the L388M variant was the most deleterious, expressing little (if any) current. Since the total Nav1.8-L388M protein in cell lysates was strongly reduced, the functional defect can readily be explained by protein instability and degradation. In support, both cellular Nav1.8 protein and current could be rescued to near wild-type levels with the proteosomal inhibitor, MG132). The L867F, P1102S and V1518I variants also led to defective Nav1.8 channels. Each of these variants expressed measureable currents, but a loss-of-function phenotype was revealed for two of the variants (L867F and V1518I) due to a positive shift in the steady-state activation curve. Thus, stronger depolarization would be needed to elicit channel opening. In contrast, a gain-of function phenotype is suggested for the P1102S variant by the slower inactivation time course, which will allow more Na^+ channel to enter the cell. The R756W variant appeared not to behave different from wild-type under our experimental conditions. Thus, with patch clamp recordings and biochemical assays, we show that four of the five rare ‘variants of unknown significance’ (L388M, L867F, P1102S and V1518I) are actually deleterious to Nav1.8 channel function.

Lack of SCN10A expression in the heart

Since *SCN10A* variants have been linked to cardiac arrhythmia disorders, it has been assumed that the gene product (the Nav1.8 channel) must be expressed in the heart. Indeed, there are reports describing the expression of *SCN10A* mRNA and Nav1.8 protein in mouse and human left ventricular myocardium.[8, 42] In one study, expression of *Scn10a* mRNA was undetectable in the mouse heart specialized cardiac conduction system when measured by qRT-PCR. [41] The same study also assessed expression in mouse ventricle by RNA-seq and found that *Scn5a* reads exceed those of *Scn10a* by 145-fold. We also detected *SCN10A*/*Scn10a* mRNA reads by RNA-seq in both human ventricle and mouse specialized cardiac conduction system, but these reads were restricted to a few exons at the 3’ end of the gene. Another study also reported RNA-seq data demonstrating the absence of full-length *Scn10a* mRNA transcripts in murine ventricle.[26] Since full-length *SCN10A* mRNA is not detected in cardiac tissue, the Nav1.8 protein cannot be an abundant cardiac channel. Indeed, we failed to detect Nav1.8 protein with immunofluorescence confocal microscopy in adult rat heart.

This observation agrees with a previous study demonstrating that Nav1.8 is not expressed in isolated mouse ventricular myocytes, but that Nav1.8 can be readily be detected in neurons from intracardiac ganglia.[43] Other studies have also found with immunohistochemistry analysis that Nav1.8 is present in nerve fibers and fascicles in the myocardium and is often closely located to small capillaries.[25] Moreover, Nav1.8 in cardiac ganglionated plexi was found to modulate arrhythmia inducibility,[44] and blocking Nav1.8 in the left stellate ganglion of dogs suppresses ventricular arrhythmia.[45] There are not many reports describing the presence of functional Nav1.8 channels in the myocardium. In one such report, the Nav1.8 blocker A-803467 was described to inhibit the "late" cardiac sodium current and can shorten action potential durations in mouse and rabbit cardiomyocytes.[46] The specificity of A-803467 to Nav1.8, however, has been questioned.[47, 48] An effect on the "late" cardiac sodium current was also demonstrated in *Scn10A* knockout mice,[26] but since these were global knockouts, the effect on the action potential may well be from extra-cardiac origins.

Can the SCN10A variants contribute to SUD?

A number of previous studies have shown that *SCN10A* variants are associated with arrhythmias,[8, 9, 11, 15–18, 27, 40, 41] but ours is the first to show to the presence of *SCN10A* VUS in cases of SUD. An association is suggested, since the chances are virtually zero of finding five *SCN10A* variants in only 330 SUD cases when the presence of these variants are undetectable or ultra-rare in a population of >250,000 individuals in the gnomAD whole-exome sequencing database. If *SCN10A* variants contributed to SUD, it would have to be from extra-cardiac sources (such as cardiac ganglia), which may alter cardiac electrophysiology and arrhythmias.

Study limitations

Although our functional studies enhance the genetic testing analysis by reclassifying 'variants of uncertain significance' as being possibly benign or potentially deleterious, by themselves they cannot be used as evidence that *SCN10A* is involved in arrhythmias or sudden death. First, we have not measured certain electrophysiological parameters such as the voltage-dependence of steady-state inactivation or recovery from inactivation. Changes in these parameters may potentially impact the apparently 'normal' R756W variant and have further detrimental effects on the L388M, L867F, P1102S and V1518I variants. Second, our studies are performed in a heterologous expression system and allowances are not made for the expression of unknown endogenous subunits, physiological temperatures and other environmental factors. Most importantly, however, is the fact that functional studies by themselves should not be used as the sole basis for determining variant pathogenicity.[49] Much stricter criteria are needed to reach such a conclusion by following the standards defined by the Clinical Genome Resource Gene Curation Working Group Standard Operating Procedures. A recent report by the NIH Clinical Genome Resource Consortium, for example, concluded that when a systematic evaluation is performed of the evidence supporting the causality of gene variants associated with Brugada syndrome, clinical validity was demonstrated for only one gene (*SCN5A*), even though over 20 genes (including *SCN10A*) have previously been implicated with Brugada syndrome.[16–18, 40, 50] To determine if *SCN10A* variants are indeed associated with SUD would require significantly more

clinical evidence, included metrics of familial or segregation data of affected cases and additional supportive functional data.

Supplementary Material

Refer to Web version on PubMed Central for supplementary material.

Acknowledgments

Funding Sources

These studies were supported in part by the National Institute of Justice (2015-DN-BX-K017; YT), the National Institutes of Health (S10 OD021589; WAC), by the Seventh Masonic District Association, Inc. (WAC) and by the American SIDS Institute (WAC).

Conceptualization (YT, GIF, IG & WAC), Data curation (IG and WAC), Formal analysis (IG and WAC), Funding acquisition (YT and WAC), Investigation (all authors), Methodology (IG and WAC), Project administration (WAC), Resources (WAC), Software (IG and WAC), Supervision (WAC and YT), Validation (WAC), Visualization (IG and WAC), Writing - original draft (IG and WAC), Writing - review & editing (all authors).

Funding Sources

These studies were supported by KiDS of NYU and by the Seventh Masonic District Association, Inc.

References

1. Wang D, Shah KR, Um SY, Eng LS, Zhou B, Lin Y, Mitchell AA, Nicaj L, Prinz M, McDonald TV, Sampson BA and Tang Y. Cardiac channelopathy testing in 274 ethnically diverse sudden unexplained deaths. Forensic Sci Int. 2014;237:90–9. [PubMed: 24631775]
2. Bagnall RD, Weintraub RG, Ingles J, Duflou J, Yeates L, Lam L, Davis AM, Thompson T, Connell V, Wallace J, Naylor C, Crawford J, Love DR, Hallam L, White J, Lawrence C, Lynch M, Morgan N, James P, du Sart D, Puranik R, Langlois N, Vohra J, Winship I, Atherton J, McGaughran J, Skinner JR and Semsarian C. A Prospective Study of Sudden Cardiac Death among Children and Young Adults. N Engl J Med. 2016;374:2441–52. [PubMed: 27332903]
3. Fernandez-Falgueras A, Sarquella-Brugada G, Brugada J, Brugada R and Campuzano O. Cardiac Channelopathies and Sudden Death: Recent Clinical and Genetic Advances. Biology. 2017;6.
4. Wilde AA and Bezzina CR. Genetics of cardiac arrhythmias. Heart. 2005;91:1352–8. [PubMed: 16162633]
5. Brugada J, Brugada R and Brugada P. Channelopathies: a new category of diseases causing sudden death. Herz. 2007;32:185–91. [PubMed: 17497250]
6. Evans A, Bagnall RD, Duflou J and Semsarian C. Postmortem review and genetic analysis in sudden infant death syndrome: an 11-year review. Hum Pathol. 2013;44:1730–6. [PubMed: 23623143]
7. Kauferstein S, Kiehne N, Jenewein T, Biel S, Kopp M, Konig R, Erkapic D, Rothschild M and Neumann T. Genetic analysis of sudden unexplained death: a multidisciplinary approach. Forensic Sci Int. 2013;229:122–7. [PubMed: 23683917]
8. Chambers JC, Zhao J, Terracciano CM, Bezzina CR, Zhang W, Kaba R, Navaratnarajah M, Lotlikar A, Sehmi JS, Kooner MK, Deng G, Siedlecka U, Parasramka S, El-Hamamsy I, Wass MN, Dekker LR, de Jong JS, Sternberg MJ, McKenna W, Severs NJ, de Silva R, Wilde AA, Anand P, Yacoub M, Scott J, Elliott P, Wood JN and Kooner JS. Genetic variation in SCN10A influences cardiac conduction. Nat Genet. 2010;42:149–52. [PubMed: 20062061]
9. Smith JG, Magnani JW, Palmer C, Meng YA, Soliman EZ, Musani SK, Kerr KF, Schnabel RB, Lubitz SA, Sotoodehnia N, Redline S, Pfeufer A, Muller M, Evans DS, Nalls MA, Liu Y, Newman AB, Zonderman AB, Evans MK, Deo R, Ellinor PT, Paltoo DN, Newton-Cheh C, Benjamin EJ, Mehra R, Alonso A, Heckbert SR, Fox ER and Candidate-gene Association Resource C. Genome-wide association studies of the PR interval in African Americans. PLoS Genet. 2011;7:e1001304. [PubMed: 21347284]

10. Holm H, Gudbjartsson DF, Arnar DO, Thorleifsson G, Thorgeirsson G, Stefansdottir H, Gudjonsson SA, Jonasdottir A, Mathiesen EB, Njolstad I, Nyrnes A, Wilsgaard T, Hald EM, Hveem K, Stoltenberg C, Lochen ML, Kong A, Thorsteinsdottir U and Stefansson K. Several common variants modulate heart rate, PR interval and QRS duration. Nat Genet. 2010;42:11722.

11. Delaney JT, Muhammad R, Shi Y, Schildcrout JS, Blair M, Short L, Roden DM and Darbar D. Common SCN10A variants modulate PR interval and heart rate response during atrial fibrillation. Europace. 2014;16:485–90. [PubMed: 24072447]

12. Butler AM, Yin X, Evans DS, Nalls MA, Smith EN, Tanaka T, Li G, Buxbaum SG, Whitsel EA, Alonso A, Arking DE, Benjamin EJ, Berenson GS, Bis JC, Chen W, Deo R, Ellinor PT, Heckbert SR, Heiss G, Hsueh WC, Keating BJ, Kerr KF, Li Y, Limacher MC, Liu Y, Lubitz SA, Marciante KD, Mehra R, Meng YA, Newman AB, Newton-Cheh C, North KE, Palmer CD, Psaty BM, Quibrera PM, Redline S, Reiner AP, Rotter JI, Schnabel RB, Schork NJ, Singleton AB, Smith JG, Soliman EZ, Srinivasan SR, Zhang ZM, Zonderman AB, Ferrucci L, Murray SS, Evans MK, Sotoodehnia N, Magnani JW and Avery CL. Novel loci associated with PR interval in a genome-wide association study of 10 African American cohorts. Circ Cardiovasc Genet. 2012;5:639–46. [PubMed: 23139255]

13. Verweij N, Mateo Leach I, Isaacs A, Arking DE, Bis JC, Pers TH, van den Berg ME, Lyytikainen LP, Barnett P, Wang X, LifeLines Cohort S, Soliman EZ, van Duijn CM, Kahonen M, van Veldhuisen DJ, Kors JA, Raitakari OT, Silva CT, Lehtimaki T, Hillege HL, Hirschhorn JN, Boyer LA, van Gilst WH, Alonso A, Sotoodehnia N, Eijgelsheim M, de Boer RA, de Bakker PI, Franke L and van der Harst P. Twenty-eight genetic loci associated with ST-T wave amplitudes of the electrocardiogram. Hum Mol Genet. 2016.

14. Iio C, Ogimoto A, Nagai T, Suzuki J, Inoue K, Nishimura K, Uetani T, Okayama H, Okura T, Shigematsu Y, Tabara Y, Kohara K, Miki T, Hamada M and Higaki J. Association Between Genetic Variation in the SCN10A Gene and Cardiac Conduction Abnormalities in Patients With Hypertrophic Cardiomyopathy. Int Heart J. 2015;56:421–7. [PubMed: 26104176]

15. Jabbari J, Olesen MS, Yuan L, Nielsen JB, Liang B, Macri V, Christophersen IE, Nielsen N, Sajadieh A, Ellinor PT, Grunnet M, Haunso S, Holst AG, Svendsen JH and Jespersen T. Common and rare variants in SCN10A modulate the risk of atrial fibrillation. Circ Cardiovasc Genet. 2015;8:64–73. [PubMed: 25691686]

16. Fukuyama M, Ohno S, Makiyama T and Horie M. Novel SCN10A variants associated with Brugada syndrome. Europace. 2015.

17. Behr ER, Savio-Galimberti E, Barc J, Holst AG, Petropoulou E, Prins BP, Jabbari J, Torchio M, Berthet M, Mizusawa Y, Yang T, Nannenberg EA, Dagradi F, Weeke P, Bastiaenan R, Ackerman MJ, Haunso S, Leenhardt A, Kaab S, Probst V, Redon R, Sharma S, Wilde A, TfeltHansen J, Schwartz P, Roden DM, Bezzina CR, Olesen M, Darbar D, Guicheney P, Crotti L, Consortium UK and Jamshidi Y. Role of common and rare variants in SCN10A: results from the Brugada syndrome QRS locus gene discovery collaborative study. Cardiovasc Res. 2015;106:520–9. [PubMed: 25691538]

18. Hu D, Barajas-Martinez H, Pfeiffer R, Dezi F, Pfeiffer J, Buch T, Betzenhauser MJ, Belardinelli L, Kahlig KM, Rajamani S, DeAntonio HJ, Myerburg RJ, Ito H, Deshmukh P, Marieb M, Nam GB, Bhatia A, Hasdemir C, Haissaguerre M, Veltmann C, Schimpf R, Borggrefe M, Viskin S and Antzelevitch C. Mutations in SCN10A are responsible for a large fraction of cases of Brugada syndrome. J Am Coll Cardiol. 2014;64:66–79. [PubMed: 24998131]

19. Akopian AN, Sivilotti L and Wood JN. A tetrodotoxin-resistant voltage-gated sodium channel expressed by sensory neurons. Nature. 1996;379:257–62. [PubMed: 8538791]

20. Sangameswaran L, Delgado SG, Fish LM, Koch BD, Jakeman LB, Stewart GR, Sze P, Hunter JC, Eglen RM and Herman RC. Structure and function of a novel voltage-gated, tetrodotoxin-resistant sodium channel specific to sensory neurons. J Biol Chem. 1996;271:5953–6. [PubMed: 8626372]

21. Shields SD, Ahn HS, Yang Y, Han C, Seal RP, Wood JN, Waxman SG and Dib-Hajj SD. Nav1.8 expression is not restricted to nociceptors in mouse peripheral nervous system. Pain. 2012;153:2017–30. [PubMed: 22703890]

22. Renganathan M, Cummins TR and Waxman SG. Contribution of Na(v)1.8 sodium channels to action potential electrogenesis in DRG neurons. J Neurophysiol. 2001;86:629–40. [PubMed: 11495938]

23. Ringkamp M, Johanek LM, Borzan J, Hartke TV, Wu G, Pogatzki-Zahn EM, Campbell JN, Shim B, Schepers RJ and Meyer RA. Conduction properties distinguish unmyelinated sympathetic efferent fibers and unmyelinated primary afferent fibers in the monkey. PLoS ONE. 2010;5:e9076. [PubMed: 20140089]
24. Gautron L, Sakata I, Udit S, Zigman JM, Wood JN and Elmquist JK. Genetic tracing of Nav1.8-expressing vagal afferents in the mouse. J Comp Neurol. 2011;519:3085–101. [PubMed: 21618224]
25. Facer P, Punjabi PP, Abrari A, Kaba RA, Severs NJ, Chambers J, Kooner JS and Anand P. Localisation of SCN10A gene product Na(v)1.8 and novel pain-related ion channels in human heart. Int Heart J. 2011;52:146–52. [PubMed: 21646736]
26. Stroud DM, Yang T, Bersell K, Kryshtal DO, Nagao S, Shaffer C, Short L, Hall L, Atack TC, Zhang W, Knollmann BC, Baudenbacher F and Roden DM. Contrasting Nav1.8 Activity in Scn10a−/− Ventricular Myocytes and the Intact Heart. Journal of the American Heart Association. 2016;5.
27. Sotoodehnia N, Isaacs A, de Bakker PI, Dorr M, Newton-Cheh C, Nolte IM, van der Harst P, Muller M, Eijgelsheim M, Alonso A, Hicks AA, Padmanabhan S, Hayward C, Smith AV, Polasek O, Giovannone S, Fu J, Magnani JW, Marciante KD, Pfeufer A, Gharib SA, Teumer A, Li M, Bis JC, Rivadeneira F, Aspelund T, Kottgen A, Johnson T, Rice K, Sie MP, Wang YA, Klopp N, Fuchsberger C, Wild SH, Mateo Leach I, Estrada K, Volker U, Wright AF, Asselbergs FW, Qu J, Chakravarti A, Sinner MF, Kors JA, Petersmann A, Harris TB, Soliman EZ, Munroe PB, Psaty BM, Oostra BA, Cupples LA, Perz S, de Boer RA, Uitterlinden AG, Volzke H, Spector TD, Liu FY, Boerwinkle E, Dominiczak AF, Rotter JI, van Herpen G, Levy D, Wichmann HE, van Gilst WH, Witteman JC, Kroemer HK, Kao WH, Heckbert SR, Meitinger T, Hofman A, Campbell H, Folsom AR, van Veldhuisen DJ, Schwienbacher C, O'Donnell CJ, Volpato CB, Caulfield MJ, Connell JM, Launer L, Lu X, Franke L, Fehrmann RS, te Meerman G, Groen HJ, Weersma RK, van den Berg LH, Wijmenga C, Ophoff RA, Navis G, Rudan I, Snieder H, Wilson JF, Pramstaller PP, Siscovick DS, Wang TJ, Gudnason V, van Duijn CM, Felix SB, Fishman GI, Jamshidi Y, Stricker BH, Samani NJ, Kaab S and Arking DE. Common variants in 22 loci are associated with QRS duration and cardiac ventricular conduction. Nat Genet. 2010;42:1068–76. [PubMed: 21076409]
28. Lin Y, Williams N, Wang D, Coetzee W, Zhou B, Eng LS, Um SY, Bao R, Devinsky O, McDonald TV, Sampson BA and Tang Y. Applying High-Resolution Variant Classification to Cardiac Arrhythmogenic Gene Testing in a Demographically Diverse Cohort of Sudden Unexplained Deaths. Circ Cardiovasc Genet. 2017;10.
29. Hellenthal N, Gaertner-Rommel A, Klauke B, Paluszkiewicz L, Stuhr M, Kerner T, Farr M, Puschel K and Milting H. Molecular autopsy of sudden unexplained deaths reveals genetic predispositions for cardiac diseases among young forensic cases. Europace. 2017;19:18811890.
30. Dewar LJ, Alcaide M, Fornika D, D'Amato L, Shafaatalab S, Stevens CM, Balachandra T, Phillips SM, Sanatani S, Morin RD and Tibbits GF. Investigating the Genetic Causes of Sudden Unexpected Death in Children Through Targeted Next-Generation Sequencing Analysis. Circ Cardiovasc Genet. 2017;10.
31. Tester DJ, Wong LCH, Chanana P, Jaye A, Evans JM, FitzPatrick DR, Evans MJ, Fleming P, Jeffrey I, Cohen MC, Tfelt-Hansen J, Simpson MA, Behr ER and Ackerman MJ. Cardiac Genetic Predisposition in Sudden Infant Death Syndrome. J Am Coll Cardiol. 2018;71:1217–1227. [PubMed: 29544605]
32. Richards S, Aziz N, Bale S, Bick D, Das S, Gastier-Foster J, Grody WW, Hegde M, Lyon E, Spector E, Voelkerding K and Rehm HL. Standards and guidelines for the interpretation of sequence variants: a joint consensus recommendation of the American College of Medical Genetics and Genomics and the Association for Molecular Pathology. Genet Med. 2015.
33. Li J, Zhao T, Zhang Y, Zhang K, Shi L, Chen Y, Wang X and Sun Z. Performance evaluation of pathogenicity-computation methods for missense variants. Nucleic Acids Res. 2018;46:7793–7804. [PubMed: 30060008]
34. Gando I, Morganstein J, Jana K, McDonald TV, Tang Y and Coetzee WA. Infant sudden death: Mutations responsible for impaired Nav1.5 channel trafficking and function. Pacing Clin Electrophysiol. 2017;40:703–712. [PubMed: 28370132]

35. Subbotina E, Williams N, Sampson BA, Tang Y and Coetzee WA. Functional characterization of TRPM4 variants identified in sudden unexpected natural death. Forensic Sci Int. 2018;293:37–46. [PubMed: 30391667]
36. Dekker LV, Daniels Z, Hick C, Elsegood K, Bowden S, Szestak T, Burley JR, Southan A, Cronk D and James IF. Analysis of human Nav1.8 expressed in SH-SY5Y neuroblastoma cells. Eur J Pharmacol. 2005;528:52–8. [PubMed: 16325806]
37. John VH, Main MJ, Powell AJ, Gladwell ZM, Hick C, Sidhu HS, Clare JJ, Tate S and Trezise DJ. Heterologous expression and functional analysis of rat Nav1.8 (SNS) voltage-gated sodium channels in the dorsal root ganglion neuroblastoma cell line ND7–23. Neuropharmacology. 2004;46:425–38. [PubMed: 14975698]
38. Schirmeyer J, Szafranski K, Leipold E, Mawrin C, Platzer M and Heinemann SH. A subtle alternative splicing event of the Na(V)1.8 voltage-gated sodium channel is conserved in human, rat, and mouse. J Mol Neurosci. 2010;41:310–4. [PubMed: 19953341]
39. Vijayaragavan K, Powell AJ, Kinghorn IJ and Chahine M. Role of auxiliary beta1-, beta2, and beta3-subunits and their interaction with Na(v)1.8 voltage-gated sodium channel. Biochem Biophys Res Commun. 2004;319:531–40. [PubMed: 15178439]
40. Bezzina CR, Barc J, Mizusawa Y, Remme CA, Gourraud JB, Simonet F, Verkerk AO, Schwartz PJ, Crotti L, Dagradi F, Guicheney P, Fressart V, Leenhardt A, Antzelevitch C, Bartkowiak S, Borggrefe M, Schimpf R, Schulze-Bahr E, Zumhagen S, Behr ER, Bastiaenen R, Tfelt-Hansen J, Olesen MS, Kaab S, Beckmann BM, Weeke P, Watanabe H, Endo N, Minamino T, Horie M, Ohno S, Hasegawa K, Makita N, Nogami A, Shimizu W, Aiba T, Froguel P, Balkau B, Lantieri O, Torchio M, Wiese C, Weber D, Wolswinkel R, Coronel R, Boukens BJ, Bezieau S, Charpentier E, Chatel S, Despres A, Gros F, Kyndt F, Lecointe S, Lindenbaum P, Portero V, Violleau J, Gessler M, Tan HL, Roden DM, Christoffels VM, Le Marec H, Wilde AA, Probst V, Schott JJ, Dina C and Redon R. Common variants at SCN5A-SCN10A and HEY2 are associated with Brugada syndrome, a rare disease with high risk of sudden cardiac death. Nat Genet. 2013;45:1044–9. [PubMed: 23872634]
41. van den Boogaard M, Smemo S, Burnicka-Turek O, Arnolds DE, van de Werken HJ, Klous P, McKean D, Muehlschlegel JD, Moosmann J, Toka O, Yang XH, Koopmann TT, Adriaens ME, Bezzina CR, de Laat W, Seidman C, Seidman JG, Christoffels VM, Nobrega MA, Barnett P and Moskowitz IP. A common genetic variant within SCN10A modulates cardiac SCN5A expression. J Clin Invest. 2014;124:1844–52. [PubMed: 24642470]
42. Dybkova N, Ahmad S, Pabel S, Tirilomis P, Hartmann N, Fischer TH, Bengel P, Tirilomis T, Ljubojevic S, Renner A, Gummert J, Ellenberger D, Wagner S, Frey N, Maier LS, Streckfuss-Bomeke K, Hasenfuss G and Sossalla S. Differential regulation of sodium channels as a novel proarrhythmic mechanism in the human failing heart. Cardiovasc Res. 2018;114:1728–1737. [PubMed: 29931291]
43. Verkerk AO, Remme CA, Schumacher CA, Scicluna BP, Wolswinkel R, de Jonge B, Bezzina CR and Veldkamp MW. Functional Nav1.8 channels in intracardiac neurons: the link between SCN10A and cardiac electrophysiology. Circ Res. 2012;111:333–43. [PubMed: 22723301]
44. Qi B, Wei Y, Chen S, Zhou G, Li H, Xu J, Ding Y, Lu X, Zhao L, Zhang F, Chen G, Zhao J and Liu S. Nav1.8 channels in ganglionated plexi modulate atrial fibrillation inducibility. Cardiovasc Res. 2014;102:480–6. [PubMed: 24419303]
45. Yu L, Wang M, Hu D, Huang B, Zhou L, Zhou X, Wang Z, Wang S and Jiang H. Blocking the Nav1.8 channel in the left stellate ganglion suppresses ventricular arrhythmia induced by acute ischemia in a canine model. Scientific reports. 2017;7:534. [PubMed: 28373696]
46. Yang T, Atack TC, Stroud DM, Zhang W, Hall L and Roden DM. Blocking Scn10a channels in heart reduces late sodium current and is antiarrhythmic. Circ Res. 2012;111:322–32. [PubMed: 22723299]
47. Stone AJ, Kim JS, Yamauchi K, Ruiz-Velasco V and Kaufman MP. Attenuation of autonomic reflexes by A803467 may not be solely caused by blockade of NaV 1.8 channels. Neurosci Lett. 2013;543:177–82. [PubMed: 23523647]
48. Han Z, Jiang Y, Xiao F, Cao K and Wang DW. The effects of A-803467 on cardiac Nav1.5 channels. Eur J Pharmacol. 2015;754:52–60. [PubMed: 25701724]

49. Gando I, Yang HQ and Coetzee WA. Functional significance of channelopathy gene variants in unexplained death. Forensic science, medicine, and pathology. 2018;293:37–46.

50. Hosseini SM, Kim R, Udupa S, Costain G, Jobling R, Liston E, Jamal SM, Szybowska M, Morel CF, Bowdin S, Garcia J, Care M, Sturm AC, Novelli V, Ackerman MJ, Ware JS, Hershberger RE, Wilde AAM and Gollob MH. Reappraisal of Reported Genes for Sudden Arrhythmic Death. Circulation. 2018;138:1195–1205. [PubMed: 29959160]

HIGHLIGHTS

- Channelopathies are often associated with inherited arrhythmias and sudden death.
- Genetic testing can assist in determining the likely causes of sudden unexpected death.
- We identified five *SCN10A* variants in sudden unexpected death.
- Four of the variants led to altered Na^+ channel function.

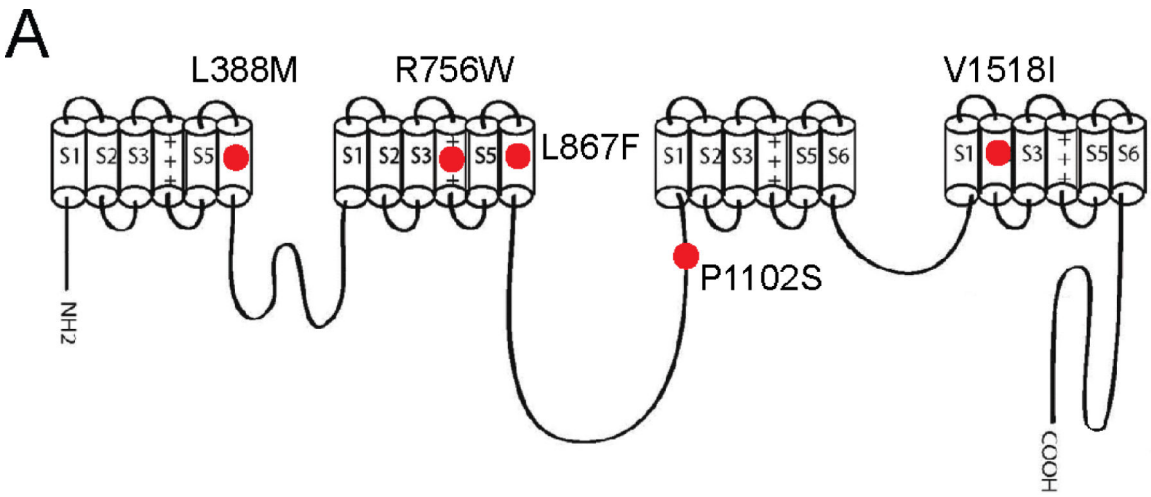

Figure 1:

Schematic topological representation of the human sodium channel α-subunit, Nav1.8. Several of the mutations fall within the transmembrane α-helical domains (L388M, R756W, L867F, V1518I) while the P1102S mutation is in the DII-DIII intracellular linker region. All the mutations occurred at evolutionarily conserved sites.

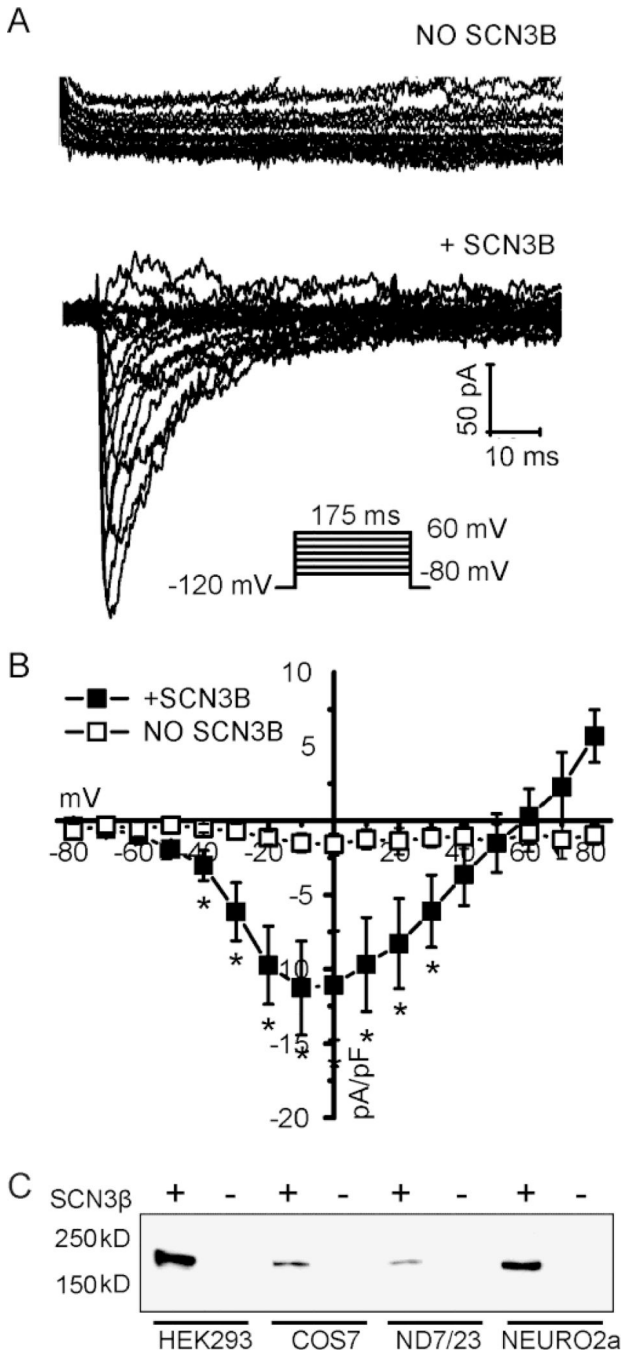

Figure 2:

Representative Nav1.8 current traces of WT channel expressed in HEK293 in the absence (A) or presence (B) of Navβ3 subunit, using the voltage protocol as shown inset in (C). The Nav1.8 current densities are plotted as a function of the test voltage (C). Data points represent mean ± SEM, with n = 7 in absence and n = 7 in the presence of Navβ3. *P < 0.05 versus wild-type (Student's t-test).

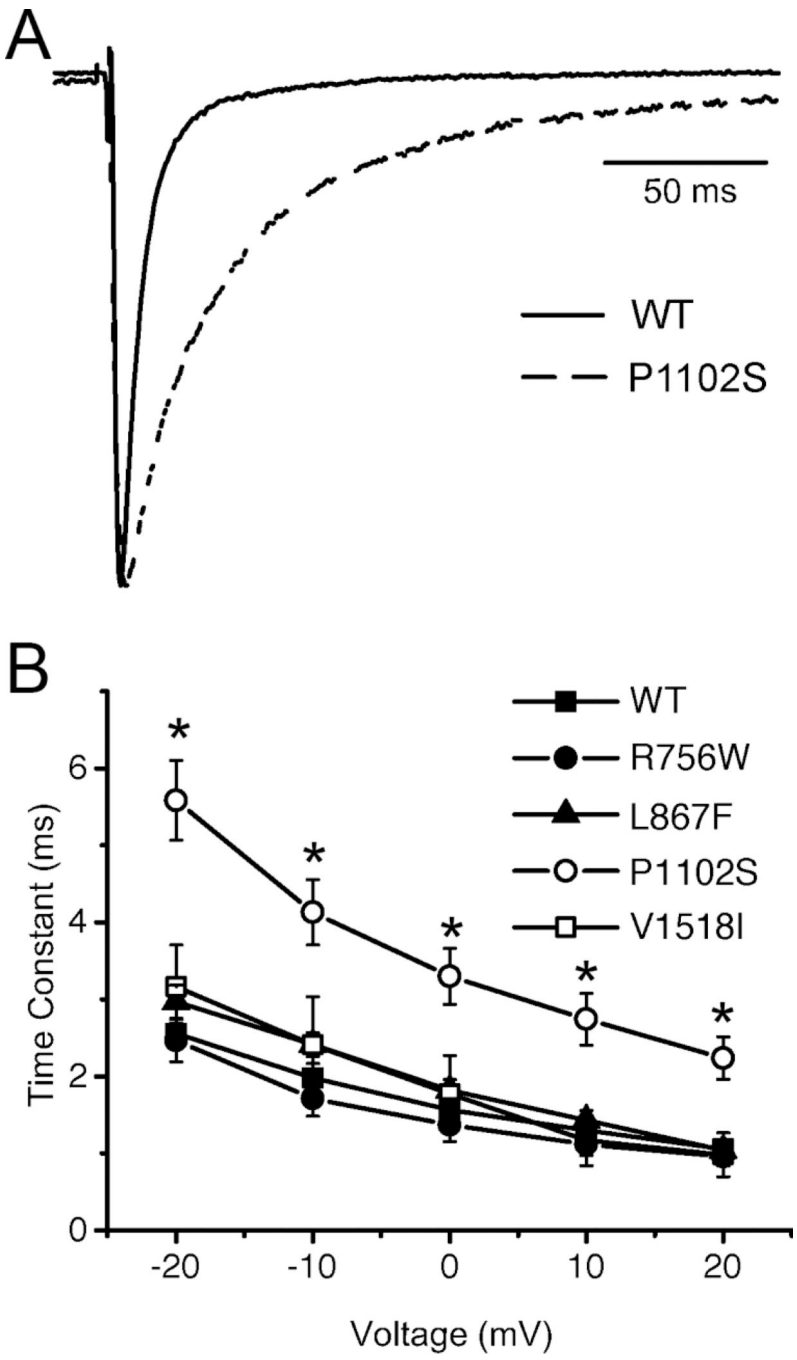

Figure 3:

Effects of *SCNA10* variants on the rate of inactivation of Nav1.8 currents (A) Representative Nav1.8 current traces of WT and P1102S channels co-expressed Navβ3 subunit in HEK293 cells. The recordings were made at 0 mV. (B) The inactivating portions of currents at −20 to +20 mV were subjected to curve fitting to a single exponential function and time constants are plotted as a function of the voltage. *P < 0.05 versus wild-type (1W-ANOVA, followed by Dunnet's t-test).

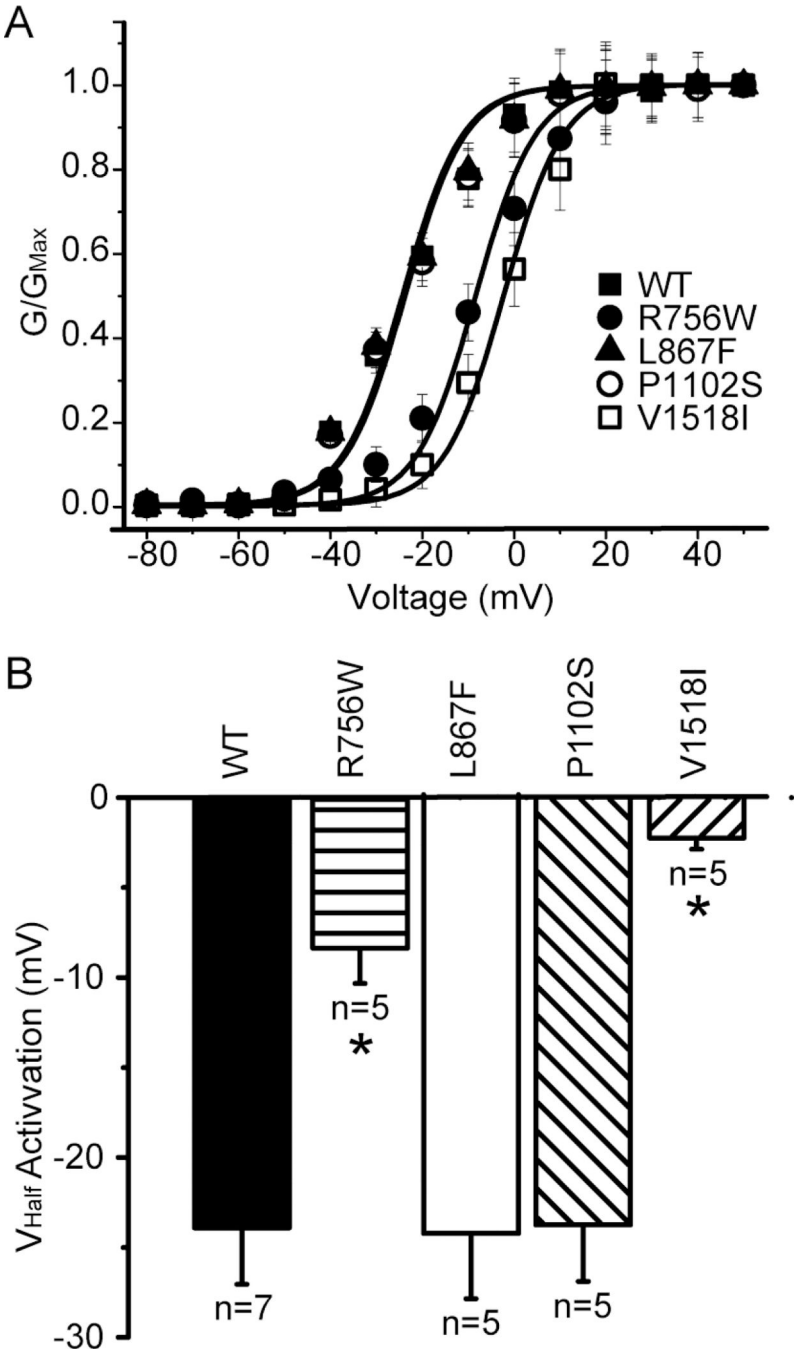

Figure 4:

Effects of *SCNA10* variants on Nav1.8 current density and total protein expressing. (A) Representative Nav1.8 current traces of WT, L388M and R756W channel co-expressed Navβ3 subunit in HEK293 cells. (B) Representative immunoblot of total proteins from HEK293 cells transfected with WT or mutant Nav1.8. Input lysates were probed with a pan-Nav antibody. GAPDH antibody was used as a protein loading control. (C) The peak currents at 0mV was normalized to the cell surface size by dividing by the cell capacitance and plotted. Compared to WT, the L388M mutant current density was significantly reduced,

−11.08 ± 3.66 pA/pF; n = 7 vs −2.43 ± 1.74 pA/pF; n=7. The R756W (−18.94 ± 5.35 pA/pF; n = 5), L867F (−14.55 ± 1.62 pA/pF; n = 5), P1102S (−19.03 ± 4.36 pA/pF; n=5) and V1518I (−12.12 ± 3.28 pA/pF; n=5) mutants all showed non-significant increased peak currents at 0 mV when compared to WT. *P < 0.05 versus wild-type (1W-ANOVA, followed by Dunnet's t-test).

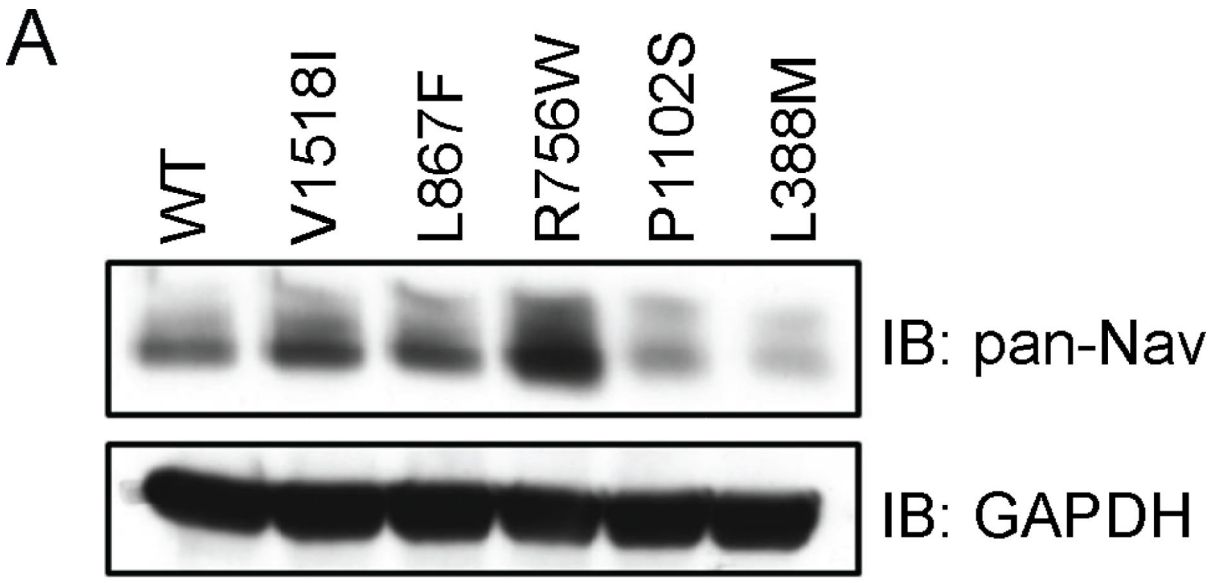

Figure 5:

(A) Steady-state activation curves for WT and mutant Nav1.8 channels. The steady-state activation curves were derived from IV curves by dividing the peak currents by the driving force (V_m-V_{Na}, with V_{Na} is the calculated equilibrium potential for Na^+ ions, which is +60mV under our experimental conditions). (B) Half-maximal voltage of steady state activation was significantly decreased in R756W (−8.37 ± 1.96 mV; n = 5) and V1518I (−2.24 ± 0.62 pA/pF; n = 5) mutants when compared to WT (−23.90 ± 3.16 mV; n = 7). *P < 0.05 versus wild-type (Student's t-test).

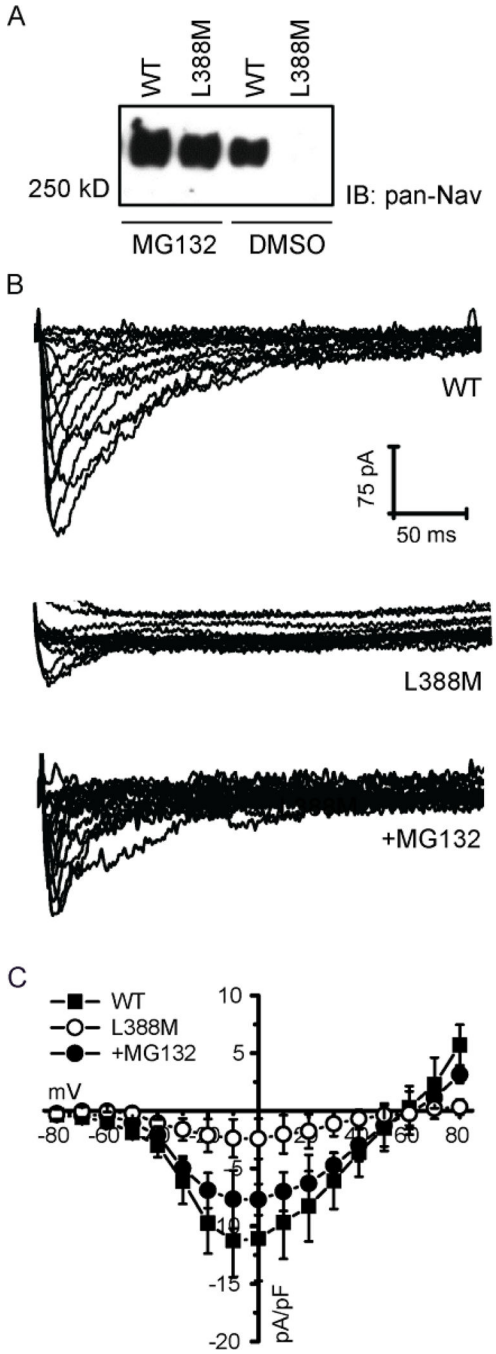

Figure 6:

(A) Representative Nav1.8 current traces of WT or L388M mutant channel with or without 24 h treatment with MG132. (B) The Nav1.8 current densities measured at voltages between −80mV to +80mV, normalized by the cell capacitance and plotted as a function of test voltage. Data points represent mean ± standard error of the mean. (C) Representative Nav1.8 immunoblot of WT and L388M mutant channel after 24 h treatment with 10UM MG132 or DMSO.

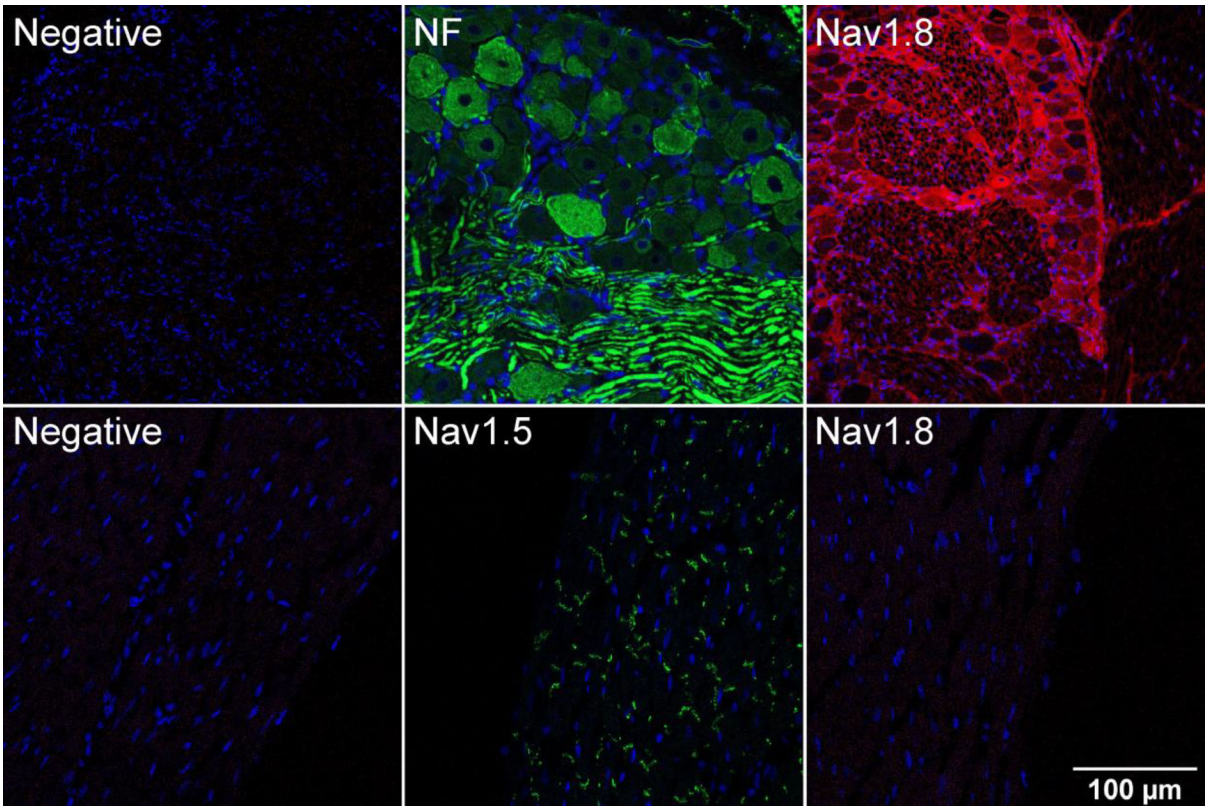

Figure 7:

Expression of Nav1.8 in rat ventricular tissue. Immunofluorescence images of adult rat DRG (top) and left ventricle (bottom) were taken using a confocal microscope. Immunostaining was performed using mouse monoclonal anti-Nav1.8 antibody followed by AlexaFlour 594 conjugated secondary antibody. Rabbit polyclonal anti-Neurofilament heavy polypeptide (NF) and anti-Nav1.5 were used as positive controls for DRG neurons and left ventricular myocytes respectively. In the negative controls for DRG and left ventricle normal donkey serum was used in place of the primary antibody. Nuclei are stained with DAPI (blue). Images were taken at 20X magnification

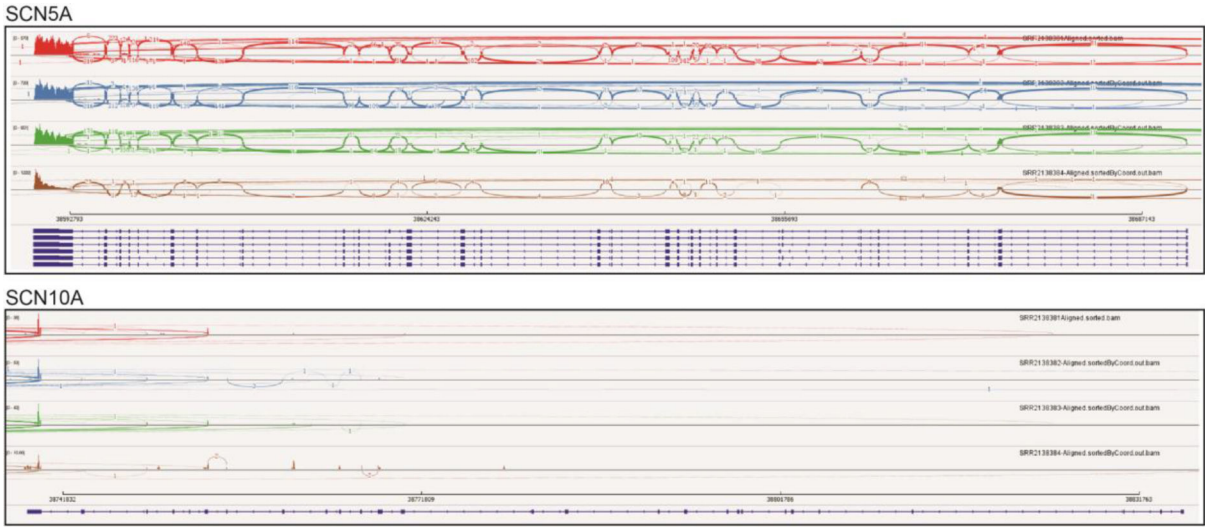

Figure 8:

RNA-seq analysis of VGSC expression in human heart. We analyzed available RNA-seq datasets obtained adult human ventricle (NCBI GEO accession: GSE71613). Shown are *SCN5A* (chr3:38,587,553–38,693,164) and *SCN10A* (chr3:38,736,837–38,837,501) mapped to the human hg19 reference build. The respective dark blue lines at the bottom of each panel represent the gene, with exons being thicker in width. Note that these two genes are anti-parallel, with exons 28 and 27 to the left respectively for *SCN5A* and *SCN10A*. The colored tracks depict Sashimi plots (reads within and spanning the exons) for the four 'control' human heart samples (SRR2138381, SRR2138382, SRR2138383 and SRR2138384). The figure was produced using Integrative Genomics Viewer v2.3.68.

Table 1:

Variants in SCN10A associated with SUD

Gene variant	Protein	Age	Classification	Sex	Ethnicity	Case Information	Incidence in gnomAD	Other variant(s)
g.38798293G>T	L388M	24 year	VUS	M	African-American	Decedent was playing in fire hydrant, collapsed and died. History of asthma. Autopsy negative	Novel	KCND3-Ala2Glu (VUS) DSP-Val2004Phe (VUS) TRPM4-Ser1143Gly (VUS)
g.38781020G>A	R756W	3 year	VUS	M	African-American	Found face down in partially filled bathtub. Recent gastrointestinal illness	6/23,972 African 9/126,154 European (Non-Finnish) 15/150,126 Total (0.01%)	None
g.38770074G>A	L867F	49 day	VUS	F	Hispanic	It was a sudden, unexpected crib death (found supine). Mother of child is 35Y old with a history of miscarriages. When she was 15Y, she had a baby who died at 2M old which was reported due to “pneumonia” at the time.	7/34,322 Latino 1/24,022 African 8/274,720 Total (0.003%)	None
g.3:38764969G>A	P1102S	2 day	VUS	M	Caucasian	Twin. Decedent was born at 38 weeks gestation. Decedent was noted to be holding his breath while eating, decedent was taken to hospital. Decedent was “floppy” with a faint pulse and agonal respirations.	1/108,936 European (Non-Finnish) 1/243,332 Total (0.0004%)	MYH7 p.Arg1344Gln
g.38743435C>T	V1518I	27 year	VUS	M	African-American	Found unresponsive in bedroom right side up by mother. Slight to moderate four chamber dilation of the heart.	14/24,032 African 1/18,864 East Asian 1/34,410 Latino 3/126,482 European (Non-Finnish) 1/6,464 Other 20/276,950 Total (0.007%)	RyR2 p.Arg3190Gln
g.38743435C>T	V1518I	2 months	VUS	F	Caucasian	Found unresponsive while co-sleeping with mother in adult bed.	See above	None

gnomAD searched on 2017–07–20. Variant classification by ACMG/AMP 2015 guidelines were made on http://wintervar.wglab.org/